

# QUARKONIUM FORMATION FROM UNCORRELATED QUARK-ANTIQUARK PAIRS

R. L. Thews

Department of Physics, University of Arizona, Tucson, AZ USA

## Abstract

The goal of this section is to assess the possibility that quarkonium production rates may be enhanced in nucleus-nucleus interactions at the LHC relative to that predicted by extrapolation of processes thought to be dominant at lower energy. This enhancement could follow from the effects of incoherent recombination mechanisms involving uncorrelated pairs of heavy quarks and antiquarks which result from multiple pair production. Two different approaches have been considered: statistical hadronization and kinetic formation. Updated predictions relevant to Pb+Pb collisions at the LHC are given.

## 1. INTRODUCTION

The utility of heavy quarkonium production rates in nuclear collisions as a signature of color deconfinement was proposed more than 15 years ago [1]. Since one expects that the long-range color confining potential will be screened in a deconfined medium, the quark and antiquark constituents of bound states will be liberated. As the system expands and cools, these constituents will, in general, diffuse away from each other to separations larger than typical hadronic dimensions. When the confining potential reappears, a given heavy quark will not be able to “find” its heavy antiquark partner and form heavy quarkonium. It must then bind with one of the antiquarks within range at hadronization. Since these antiquarks are predominantly the lighter  $u$ ,  $d$ , and  $s$  flavors, the final hadronic states will preferentially be those with “open” heavy flavor. The result will be a decreased population of heavy quarkonium relative to that which would have formed if a region of deconfinement had not been present. This scenario as applied to the charm sector is known as  $J/\psi$  suppression.

At LHC energy, perturbative QCD estimates predict that hundreds of pairs of charm-anticharm quarks will be produced in a central lead-lead collision. This situation provides a “loophole” in the Matsui-Satz argument since there will be copious numbers of heavy antiquarks in the interaction region with which any given heavy quark may combine. In order for this to happen, however, one must invoke a physical situation in which quarkonium states can be formed from *all combinations* of heavy quarks and antiquarks. This of course would be expected to be valid in the case that a space-time region of color deconfinement is present but it is not necessarily limited to this possibility.

One can make a model-independent estimate of how such a “recombination” mechanism would depend on nuclear collision observables. For a given charm quark, the probability  $\mathcal{P}$  to form a  $J/\psi$  is proportional to the number of available anticharm quarks relative to the number of light antiquarks,

$$\mathcal{P} \propto \frac{N_{\bar{c}}}{N_{\bar{u}, \bar{d}, \bar{s}}} \propto \frac{N_{c\bar{c}}}{N_{\text{ch}}} . \quad (1)$$

In the second step, we have replaced the number of available anticharm quarks by the total number of pairs initially produced, assuming that the total number of bound states formed remains a small fraction of the total  $c\bar{c}$  production. We normalize the number of light antiquarks by the number of produced charged hadrons. Since this probability is generally very small, one can simply multiply by the total number of charm quarks,  $N_c$ , to obtain the number of  $J/\psi$  expected in a given event,

$$N_{J/\psi} \propto \frac{N_{c\bar{c}}^2}{N_{\text{ch}}} , \quad (2)$$

where the use of the initial values  $N_{c\bar{c}} = N_c = N_{\bar{c}}$  is again justified by the relatively small number of bound states formed.

The essential property of this result is that the growth of  $N_{J/\psi}$ , quadratic in total charm, with energy [2] is expected to be much faster than the growth of total particle production in heavy ion collisions [3]. Without this quadratic mechanism,  $J/\psi$  production is typically some small energy-independent fraction of total initial charm production [4]. We thus anticipate that the quadratic formation will become dominant at sufficiently high energy. Generic estimates of the significance of this type of formation process can be made [5]. Here we look at specific predictions of two models which share the above properties and update the expectations to LHC energies.

## 2. Statistical Hadronization

The statistical hadronization model is motivated by the successful fits of relative abundances of light hadrons produced in high energy heavy ion interactions according to a hadron gas in chemical and thermal equilibrium [6]. Extension of the model to hadrons containing heavy quarks underpredicts the observed abundances. This effect may be attributed to the long time scales associated with thermal production and annihilation of heavy quarks. The statistical hadronization model as first formulated for charm quarks [7] assumes that the  $c\bar{c}$  pairs produced in the initial hadronic interactions survive until their subsequent hadronization, at which time they are distributed into hadrons according to the same thermal equilibrium parameters that fit the light hadron abundances. Chemical equilibrium abundances are adjusted by a factor  $\gamma_c$  which accounts for the non-thermal heavy quark density. One power of this factor multiplies a given thermal hadron population for each heavy quark or antiquark contained in the hadron. Thus the relative abundance of the  $J/\psi$  to that of  $D$  mesons, for example, may be enhanced in this model.

The value of  $\gamma_c$  is determined by conservation of the heavy quark flavor. For the charm sector, the conservation constraint relates the number of initially-produced  $c$ - $\bar{c}$  pairs  $N_{c\bar{c}}$  to their distribution into open and hidden charm hadrons,

$$N_{c\bar{c}} = \frac{1}{2}\gamma_c N_{\text{open}} + \gamma_c^2 N_{\text{hidden}}, \quad (3)$$

where  $N_{\text{open}}$  is the number of hadrons containing one  $c$  or  $\bar{c}$  quark and  $N_{\text{hidden}}$  is the number of hadrons containing a  $c\bar{c}$  pair. For most applications,  $N_{\text{hidden}}$  (and also multi-charm hadrons) can be neglected compared with  $N_{\text{open}}$  due to the mass differences. Thus the charm enhancement factor is simply

$$\gamma_c = \frac{2N_{c\bar{c}}}{N_{\text{open}}}, \quad (4)$$

leading directly to the quadratic dependence of the hidden charm hadron population on  $N_{c\bar{c}}$ . One can then express the total number of  $J/\psi$  in terms of the various thermal densities,  $n_i$ , and the total number of  $c\bar{c}$  pairs,  $N_{c\bar{c}}$ . One factor of system volume  $V$  remains implicit here. It is generally replaced by the ratio of number to density for total charged hadrons,  $n_{\text{ch}}/N_{\text{ch}}$ . Then the number of  $J/\psi$  produced obeys the generic form anticipated in Eq. (2).

$$N_{J/\psi} = 4 \frac{n_{\text{ch}} n_{J/\psi}}{n_{\text{open}}^2} \frac{N_{c\bar{c}}^2}{N_{\text{ch}}} \quad (5)$$

For collider experiments such as those at the LHC and RHIC, relating the corresponding central rapidity densities will be more relevant. Since Eq. (5) is homogeneous in the total particle and quark pair numbers, it will also be valid if these are replaced by their rapidity densities. To get an order of magnitude estimate, we choose a “standard” set of thermal parameters,  $T = 170$  MeV and  $\mu_B \approx 0$ , for which the thermal density ratio is approximately 0.5. For a specific normalization, we assume  $dN_{\text{ch}}/dy$

= 2000 for a central collision at the LHC and take the initial charm rapidity density to be  $dN_{c\bar{c}}/dy = 25$ , roughly corresponding to  $N_{c\bar{c}} = 200$  for central collisions ( $b = 0$ ). Using these inputs, one predicts  $dN_{J/\psi}/dy = 0.625$ , indicating that several  $J/\psi$  will form through statistical hadronization in a central collision. To put this number in perspective, it is revealing to form the  $J/\psi$  to  $N_{c\bar{c}}$  rapidity density ratio, 0.025 with the same assumptions. For comparison, one expects the corresponding hadronic production ratio to be of 0.01. This number would then be significantly reduced if placed in a region of color deconfinement. Thus the efficiency of  $J/\psi$  formation via statistical hadronization at the LHC is expected to be substantial.

These numbers can be easily adjusted to other charm and charged particle densities using Eq. (5). Variations of the thermal parameters can also be investigated. For example, if the hadronization temperature is decreased to 150 MeV, the prefactor combination of thermal densities increases by approximately a factor of two.

The centrality dependence is controlled by the behavior of  $N_{c\bar{c}}$  and  $N_{ch}$ . The former should be proportional to the nuclear overlap function  $T_{AA}(b)$  but is generally recast in terms of the dependence on the number of nucleon participants,  $N_{part}$ . The calculation of  $N_{part}$  requires a model calculation dependent on the total inelastic cross section,  $\sigma_{in}$ , as well as the nuclear geometry. We parameterize the expected behavior as a power-law  $N_{c\bar{c}} \propto N_{part}^{4/3}$ . However, there will be deviations from this behavior for the larger values of  $\sigma_{in}$  expected at the LHC [8]. The centrality dependence of  $N_{ch}$  at RHIC is also consistent with a power-law with exponent  $\approx 1.2$  [3, 9]. We will use the same dependence for our estimates at the LHC. It is clear that for sufficiently peripheral collisions one will encounter situations in which the average number of initially produced  $c\bar{c}$  pairs is of order unity or less. At this point, one must revisit the assumptions of the original statistical hadronization model which assumed a grand canonical ensemble. The grand canonical approach is valid only when  $N_{c\bar{c}}$  is large enough for the fluctuations about the average value to be negligible. Thus for peripheral collisions, one must recalculate the statistical results in the canonical approach where the charm number is exactly conserved, as noted in [10]. Charm conservation can be implemented via a correction factor [11],

$$N_{c\bar{c}} = \frac{1}{2}\gamma_c N_{open} \frac{I_1(\gamma_c N_{open})}{I_0(\gamma_c N_{open})} + \gamma_c^2 N_{hidden}. \quad (6)$$

In the limit of large  $\gamma_c N_{open}$ , the ratio of Bessel functions approaches unity and the grand canonical result is recovered. In the opposite limit when  $\gamma_c N_{open} \rightarrow 0$ , the ratio of Bessel functions approaches  $\frac{1}{2}\gamma_c N_{open}$ . In this limit, the dependence on  $N_{c\bar{c}}$  in Eq. (5) changes from quadratic to linear. At the LHC this effect will not be relevant until one reaches very peripheral events, but at lower energies it can be significant over a much larger range of centralities [12].

The results for  $dN_{J/\psi}/dy$  as a function of  $N_{part}$  at the LHC are shown in Fig. 1. The results are shown for three different values of  $dN_{c\bar{c}}/dy(b = 0)$ , corresponding to  $N_{c\bar{c}}(0) \approx 200, 150$ , and 100. There is a rapid increase with centrality due to the quadratic dependence of  $N_{J/\psi}$  on  $N_{c\bar{c}}$ .

It is also interesting to look at these results normalized by  $N_{part}$ , shown in Fig. 2. This ratio also increases with centrality, providing a signature for the statistical hadronization process that is less dependent on  $N_{c\bar{c}}$  for the overall normalization. The corresponding results when normalized by  $dN_{c\bar{c}}/dy$  are shown in Fig. 3. The same general behavior is seen but the increase with centrality is less pronounced since the  $dN_{c\bar{c}}/dy$  is assumed to vary with a larger power,  $N_{part}^{4/3}$ . All of these ratios are at the percent level for central collisions and hence are larger than expected if the total  $J/\psi$  population were due to initial production followed by suppression in a deconfined medium.

The region of very peripheral collisions deserves some separate comments. First, there is a rise at low  $N_{part}$  in both Figs. 2 and 3 due to the onset of corrections from the canonical ensemble treatment. However, the extremely large values of the ratios as  $N_{part} \rightarrow 0$  are an artifact of the decreasing interaction volume,  $V \rightarrow 0$ . This calculation must be cut off before  $N_{part} = 2$ , i.e. only one interacting pair. It is also in this region where one must take into account the remaining  $J/\psi$  from initial production.

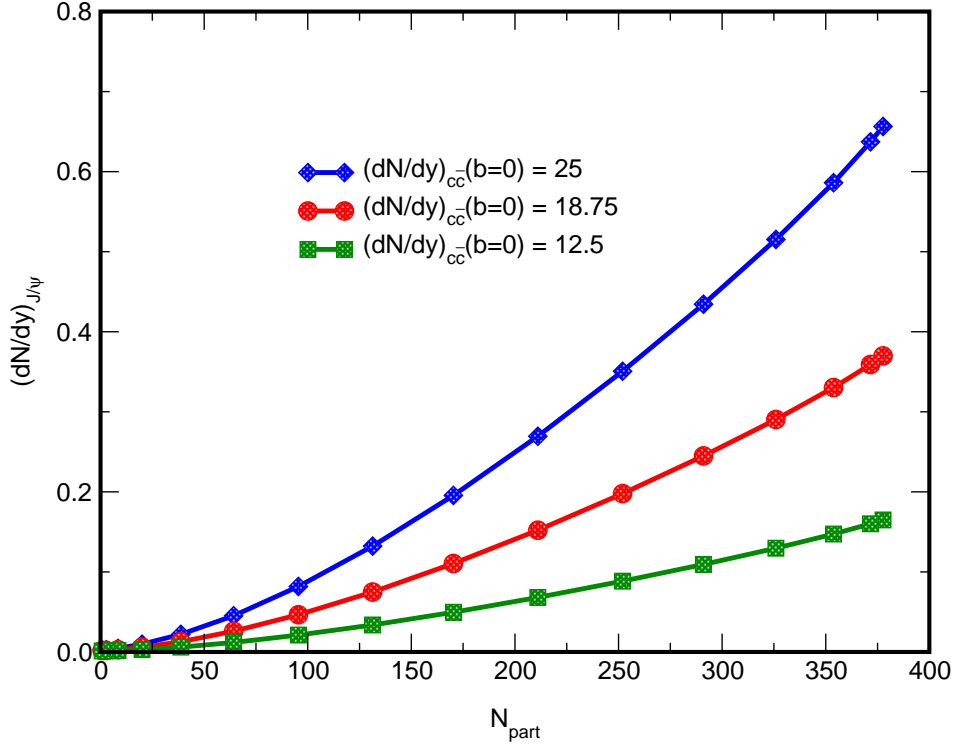


Fig. 1: Statistical hadronization results for  $J/\psi$  production as a function of  $N_{\text{part}}$  at the LHC.

Since the survival probability is maximum for very peripheral collisions and the statistical hadronization process is least effective in this same region, there will be a crossover in the relative importance of the two mechanisms. Some studies have already been performed for this situation at SPS and RHIC energies [13, 14, 15].

Finally, there is another lower cutoff in centrality for the statistical hadronization results, needed to avoid a contradiction with the  $\psi/(J/\psi)$  ratio at the SPS. Since both of these states receive identical factors of  $\gamma_c$ , their ratio must be that predicted for chemical equilibrium in the absence of any charm enhancement or suppression. Although the measured ratio appears to be consistent for more central collisions [16], there is an indication that it rises sharply for more peripheral collisions. Most treatments have thus inserted a cutoff of  $N_{\text{part}} = 100$ , below which model predictions become inconsistent [7].

The numerical values for  $dN_{J/\psi}/dy$  are tabulated as a function of impact parameter in Table 1 for the three choices of initial charm multiplicity density and the default values of all other quantities.

### 3. Kinetic Formation in a Deconfined Region

The kinetic model has been developed [17, 18] to investigate the possibility that  $J/\psi$  may form directly in a deconfined medium. This formation takes advantage of the mobility of the initially-produced charm quarks in a deconfined region. In order to motivate this view, consider the “standard” physical picture of deconfinement in which quarkonium is suppressed by collisions with free gluons in the medium [19]. Then the formation process, in which a  $c$  and  $\bar{c}$  in a relative color octet state are captured into a color-singlet quarkonium bound state and emit a color octet gluon, is simply the inverse of the breakup reaction responsible for the suppression. This is an inevitable consequence of the suppression picture.

The proper time evolution of the  $J/\psi$  population is given by the rate equation

$$\frac{dN_{J/\psi}}{d\tau} = \lambda_F \frac{N_c N_{\bar{c}}}{V(\tau)} - \lambda_D N_{J/\psi} \rho_g, \quad (7)$$

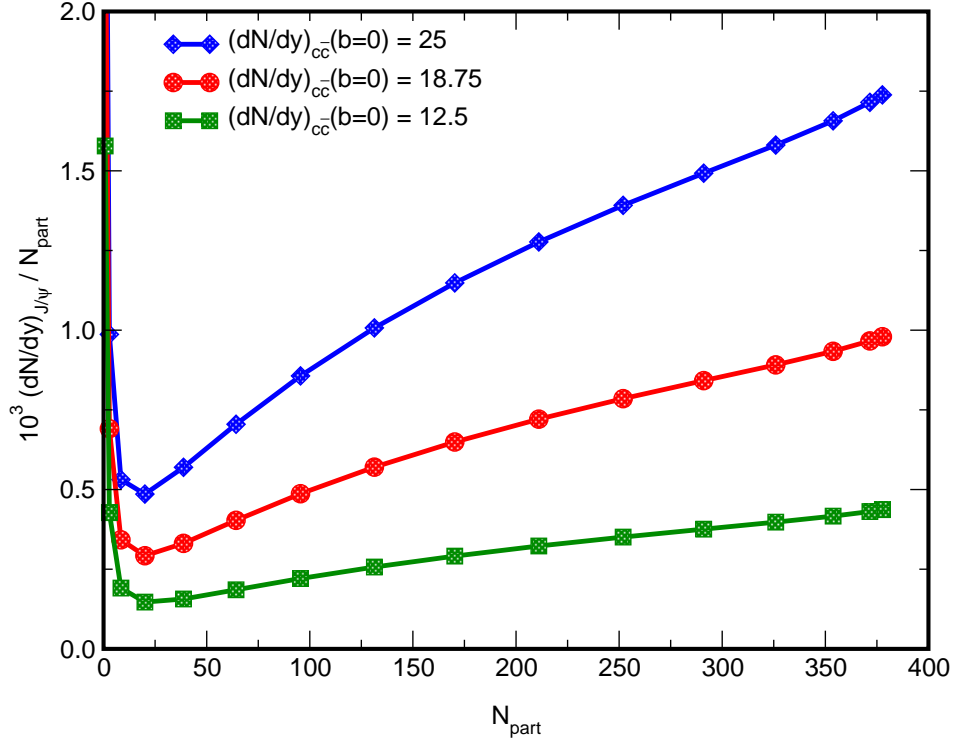


Fig. 2: The statistical hadronization results divided by  $N_{\text{part}}$  as a function of  $N_{\text{part}}$ .

where  $\rho_g$  is the gluon number density and  $V(\tau)$  is the time-dependent volume of the deconfined spatial region. The reactivities  $\lambda_{F,D}$  are the reaction rates,  $\langle \sigma v_{\text{rel}} \rangle$ , averaged over the momentum distributions of the initial participants, i.e.  $c$  and  $\bar{c}$  for  $\lambda_F$  and  $J/\psi$  and  $g$  for  $\lambda_D$ .

The solution of Eq. (7) grows quadratically with  $N_{c\bar{c}}$ , as long as  $N_{J/\psi} \ll N_{c\bar{c}}$ . In this case, we have

$$N_{J/\psi}(\tau_f) = \epsilon(\tau_f) \left[ N_{J/\psi}(\tau_0) + N_{c\bar{c}}^2 \int_{\tau_0}^{\tau_f} d\tau \lambda_F [V(\tau) \epsilon(\tau)]^{-1} \right]. \quad (8)$$

The function  $\epsilon(\tau_f) = \exp(-\int_{\tau_0}^{\tau_f} d\tau \lambda_D \rho_g)$  would be the suppression factor if formation were neglected.

The quadratic factor  $N_{c\bar{c}}^2$  is present, as expected, for the additional formation process. The normalization factor of  $N_{\text{ch}}$  is not immediately evident, but is implicit in the system volume factor. This volume is now time-dependent, accounting for the decreasing charm quark density during expansion. Here the transverse area of the deconfined region is determined not just by the nuclear geometry but by the dynamics which determine the extent of the deconfined region. This area is modeled by the energy density in terms of the local participant density in the transverse plane,  $n_{\text{part}}(b, s=0)$ . The transverse area is defined by the ratio of the participant number to the local participant density. Note that the maximum local density is at  $s=0$ . Thus,

$$A_T(b) = A_T(0) [N_{\text{part}}(b) n_{\text{part}}(0, s=0) / N_{\text{part}}(0) n_{\text{part}}(b, s=0)] \quad (9)$$

These area effects will be more explicit when the centrality dependence is considered.

The numerical results depend on a number of parameters, including the initial volume and temperature, the time expansion profile, the reaction cross sections, the behavior of the quarkonium masses and binding energies in the deconfined region, and the charm quark momentum distributions. For specifics, see Ref. [20]. Our previous results have used initial values  $N_{c\bar{c}} = 200, 150$ , and  $100$ , spanning a reasonable range of expectations [21]. The results are very sensitive to the initial charm quark momentum

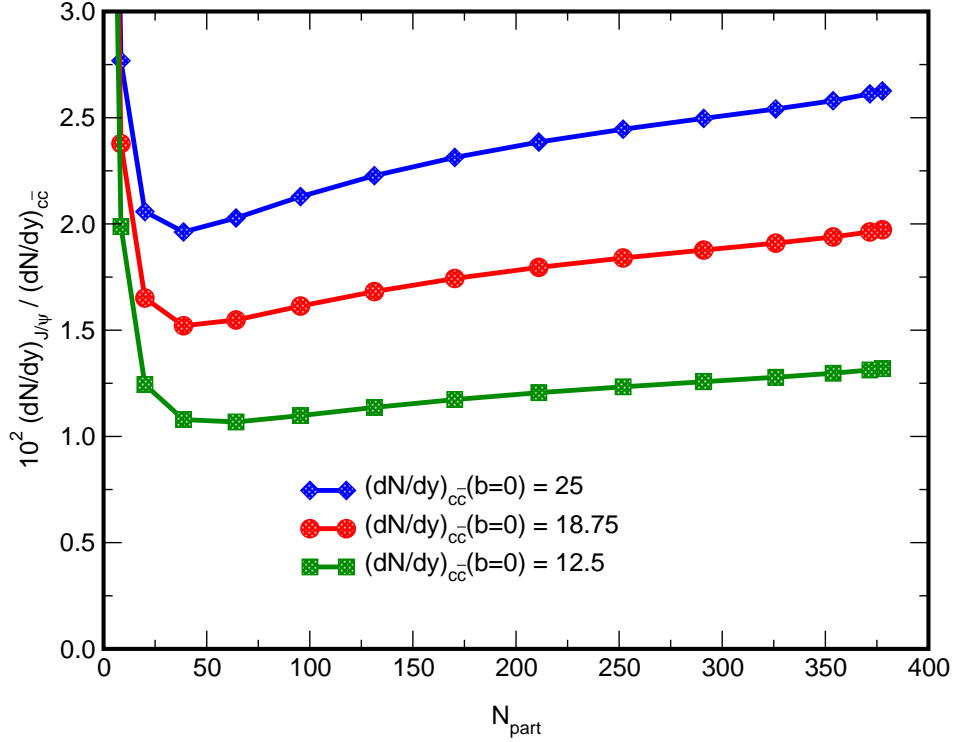


Fig. 3: The statistical hadronization results for  $J/\psi$  production at the LHC, divided by the open charm multiplicity,  $dN_{c\bar{c}}/dy$ , as a function of  $N_{\text{part}}$ .

distributions, as may be expected. We assume the charm  $p_T$  distributions are gaussian and the charm rapidity distributions are flat over a plateau of variable width,  $\Delta y$ . The range  $1 < \Delta y < 7$  spans the range between an approximate thermal momentum distribution,  $\Delta y \approx 1$ , to a distribution similar to that of the initial pQCD production,  $\Delta y \approx 7$ .

The results as a function of the initial number of  $c\bar{c}$  pairs produced in central collisions are shown in Fig. 4. There is a rapid decrease in formation with increasing  $\Delta y$ . The quadratic dependence on  $N_{c\bar{c}}$  is evident, but there is also a substantial linear component in some of the curves. This linear contribution arises because the final  $J/\psi$  formation by this mechanism is large enough for exact charm conservation to reduce the number of  $c$  and  $\bar{c}$  quarks available to participate in the formation process. The curve labeled “Quadratic Extrapolation” uses a quadratic dependence derived from a fit valid only for low  $N_{c\bar{c}}$ . Note that the result for a thermal distribution is very similar to the assumption  $\Delta y = 1$ .

The corresponding centrality dependence is presented in Fig. 5, where we give  $N_{J/\psi}$  at hadronization for three different initial charm quark momentum distributions, thermal,  $\Delta y = 4$  and  $\Delta y = 7$ , as well as for our three choices of  $N_{c\bar{c}}(b = 0)$ .

Finally, the ratio of final  $J/\psi$  to initial charm production is shown in Fig. 6 using the same parameters in Fig. 4. These ratios are most easily compared to either initial production or suppression. There is a substantial variation in the predictions and it is evident that a simultaneous measurement of open charm will be required for an interpretation. However, the centrality dependence is opposite to that expected in any pure suppression scenario.

We have updated the calculations to include the charm quark momentum distribution from a leading order pQCD calculation [22]. The rapidity distribution has a somewhat larger effective  $\Delta y$  and the  $p_T$  distribution does not fall as fast as a simple gaussian. As a result, the formation efficiency is further reduced. Such distributions may be most relevant, given preliminary results from RHIC [23, 24].

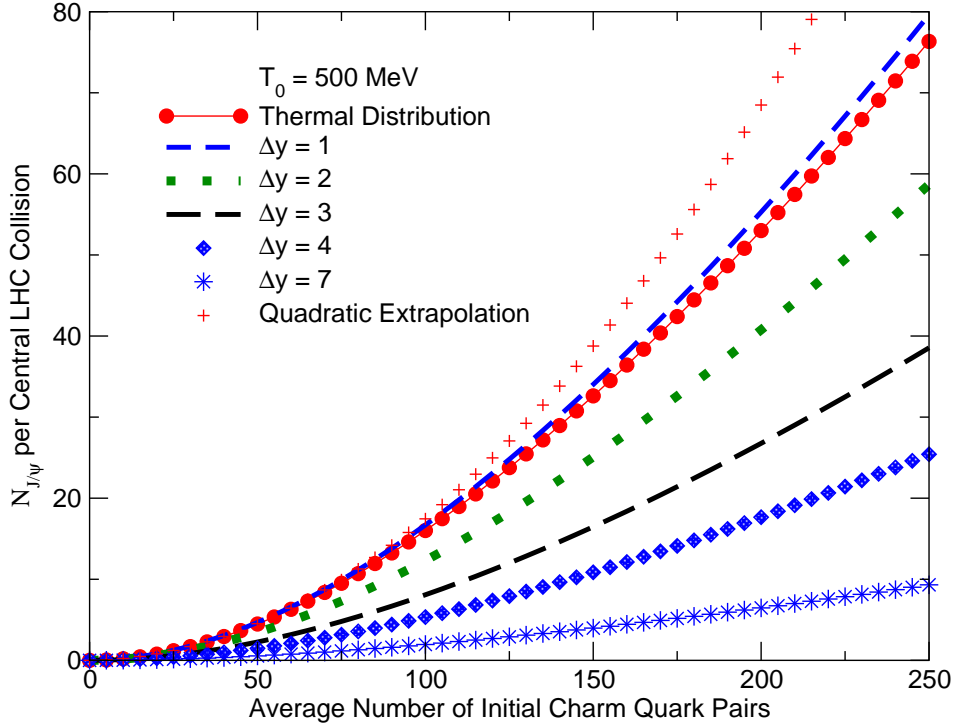


Fig. 4: The  $J/\psi$  production per central LHC collision in the kinetic model as a function of the initial number of  $c\bar{c}$  pairs.

The numerical values for  $N_{J/\psi}$  are compared with the statistical hadronization model results for  $dN_{J/\psi}/dy$  in Table 1. The overall magnitudes are comparable, although the centrality dependences differ somewhat. Thus details such as the resulting  $J/\psi$  momentum distributions will be required to differentiate between these two models [22]. For completeness,  $N_{J/\psi}$  for the thermal distributions and the assumption  $\Delta y = 4$  are presented in Table 2.

#### 4. Conclusions

The "smoking gun" signature of the quarkonium formation mechanism is the quadratic dependence on total charm. For central collisions at the LHC one expects that this feature will lead to a total  $J/\psi$  rate greater than that produced by an incoherent superposition of the initial nucleon-nucleon collisions, even without any subsequent suppression due to deconfinement effects. In addition, the centrality dependence can be used to identify the quadratic dependence on charm assuming that the initial charm production scales with the number of binary collisions. Binary scaling leads to an increase of the ratio of  $J/\psi$  to initial charm as the collision centrality increases, independent of specific parameters which control the overall magnitudes. A simultaneous measurement of total charm will be essential for such conclusions to be drawn.

Uncertainties in the absolute magnitude of the formation process are inherent in the model parameters. For statistical hadronization, one can constrain the thermal parameters to within a factor of two using the observed hadron populations. There is some additional uncertainty related to the lower cutoff on centrality needed to ensure the quarkonium ratios are consistent with an overall thermal picture. There is also the possibility that the correction for canonical ensemble effects will involve a thermal volume parameter not necessarily equal to the total system volume [25]. In addition, the formation mechanism could be limited to those charm quarks whose phase space separation is within some maximum value, introducing another as yet unconstrained parameter [14]. With kinetic formation, a similar set of uncertainties exist. There are uncertainties in the space-time properties of the deconfinement region. In

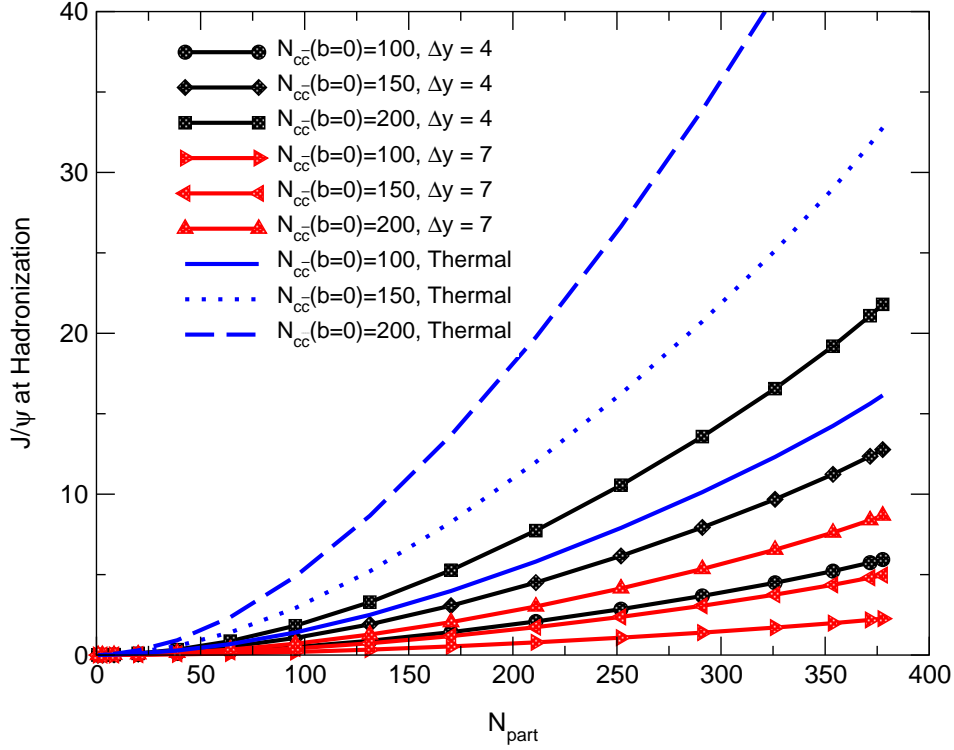


Fig. 5: The centrality dependence of  $J/\psi$  production in the kinetic model.

addition, possible variations of charmonium binding energies and reaction cross sections in a deconfined region are at present not well understood. There are indications that the efficiency of the formation mechanism is considerably reduced when included in a partonic transport calculation [26].

The primary uncertainty in both models is still the initial number of charm quarks and their momentum distributions. The tabulated  $J/\psi$  results should be regarded in this light. Thus numbers may be only an order of magnitude estimate. However, the variation with centrality and total initial charm should provide experimental signatures which are largely independent of the overall magnitudes.

## 5. Acknowledgments

My thanks to Anton Andronic for discussions on the Statistical Model and Martin Schroedter for updates on the Kinetic Model calculations. This work was supported in part by U.S. Department of Energy Grant DE-FG03-95ER40937.

## References

- [1] T. Matsui and H. Satz, Phys. Lett. B **178** (1986) 416.
- [2] P. L. McGaughey, E. Quack, P. V. Ruuskanen, R. Vogt and X. N. Wang, Int. J. Mod. Phys. A **10** (1995) 2999 [arXiv:hep-ph/9411438].
- [3] A. Bazilevsky [the PHENIX Collaboration], arXiv:nucl-ex/0209025.
- [4] R. Gavai, D. Kharzeev, H. Satz, G. A. Schuler, K. Sridhar and R. Vogt, Int. J. Mod. Phys. A **10** (1995) 3043 [arXiv:hep-ph/9502270].



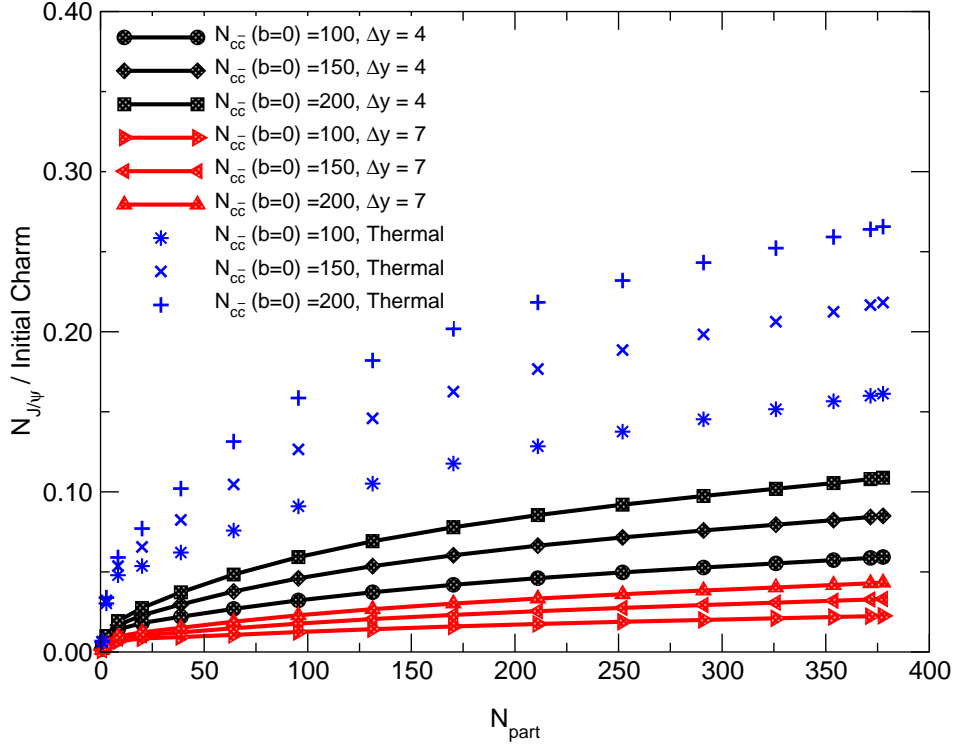


Fig. 6: The ratio of the number of produced  $J/\psi$ 's in the kinetic model to the initial number of  $c\bar{c}$  pairs as a function of  $N_{\text{part}}$ .

- [5] R. L. Thews, Nucl. Phys. A **702** (2002) 341 [arXiv:hep-ph/0111015].
- [6] P. Braun-Munzinger, D. Magestro, K. Redlich and J. Stachel, Phys. Lett. B **518** (2001) 41 [arXiv:hep-ph/0105229].
- [7] P. Braun-Munzinger and J. Stachel, Phys. Lett. B **490** (2000) 196 [arXiv:nucl-th/0007059].
- [8] A. Andronic, P. Braun-Munzinger, K. Redlich and J. Stachel, arXiv:nucl-th/0209035.
- [9] D. Kharzeev, E. Levin and M. Nardi, arXiv:hep-ph/0111315.
- [10] M. I. Gorenstein, A. P. Kostyuk, H. Stocker and W. Greiner, Phys. Lett. B **509** (2001) 277 [arXiv:hep-ph/0010148].
- [11] J. Cleymans, K. Redlich and E. Suhonen, Z. Phys. C **51** (1991) 137.
- [12] M. I. Gorenstein, A. P. Kostyuk, H. Stocker and W. Greiner, Phys. Lett. B **524** (2002) 265 [arXiv:hep-ph/0104071].
- [13] L. Grandchamp and R. Rapp, arXiv:hep-ph/0209141.
- [14] L. Grandchamp and R. Rapp, Nucl. Phys. A **709** (2002) 415 [arXiv:hep-ph/0205305].
- [15] L. Grandchamp and R. Rapp, Phys. Lett. B **523** (2001) 60 [arXiv:hep-ph/0103124].
- [16] H. Sorge, E. V. Shuryak and I. Zahed, Phys. Rev. Lett. **79** (1997) 2775 [arXiv:hep-ph/9705329].
- [17] R. L. Thews, M. Schroedter and J. Rafelski, Phys. Rev. C **63** (2001) 054905 [arXiv:hep-ph/0007323].

Table 1: Comparison of  $J/\psi$  production at the LHC by the statistical hadronization (left-hand side) and kinetic formation (right-hand side) models.

	$dN_{J/\psi}/dy$ (Statistical) $dN_{c\bar{c}}(0)/dy$			$N_{J/\psi}$ (Kinetic, LO Charm) $N_{c\bar{c}}(0)$		
$b$ (fm)	25	18.75	12.5	200	150	100
0	0.656	0.370	0.165	4.0	2.26	1.03
1	0.637	0.359	0.160	3.85	2.19	1.00
2	0.586	0.330	0.147	3.51	2.00	0.91
3	0.515	0.290	0.130	3.04	1.73	0.79
4	0.434	0.245	0.109	2.50	1.43	0.65
5	0.351	0.198	0.088	1.97	1.12	0.51
6	0.270	0.152	0.068	1.46	0.84	0.38
7	0.196	0.110	0.050	1.01	0.58	0.27
8	0.132	0.075	0.034	0.65	0.38	0.18
9	0.082	0.046	0.021	0.38	0.22	0.10
10	0.045	0.026	0.012	0.20	0.12	0.057
11	0.022	0.013	0.0061	0.087	0.054	0.028
12	0.0097	0.0058	0.0029	0.034	0.022	0.012
13	0.0045	0.0029	0.0016	0.011	0.0075	0.0041
14	0.0028	0.0019	0.0012	0.0021	0.0013	$6.8 \times 10^{-4}$
15	0.0025	0.0018	0.0012	$1.8 \times 10^{-4}$	$1.0 \times 10^{-4}$	$5.1 \times 10^{-5}$

- [18] R. L. Thews and J. Rafelski, Nucl. Phys. A **698** (2002) 575 [arXiv:hep-ph/0104025].
- [19] D. Kharzeev and H. Satz, Phys. Lett. B **334** (1994) 155 [arXiv:hep-ph/9405414].
- [20] R. L. Thews, Published in the proceedings of Pan American Advanced Studies Institute: New States of Matter in Hadronic Interactions (PASI 2002), Campos do Jordao 2002, 490 [arXiv:hep-ph/0206179].
- [21] R. Vogt [Hard Probe Collaboration], arXiv:hep-ph/0111271.
- [22] M. L. Mangano and R. L. Thews, in progress.
- [23] K. Adcox *et al.* [PHENIX Collaboration], Phys. Rev. Lett. **88** (2002) 192302 [arXiv:nucl-ex/0201008].
- [24] A. D. Frawley, [PHENIX Collaboration], [arXiv:nucl-ex/0210013]
- [25] K. Redlich and A. Tounsi, Eur. Phys. J. C **24** (2002) 589 [arXiv:hep-ph/0111261].
- [26] B. Zhang, C. M. Ko, B. A. Li, Z. W. Lin and S. Pal, Phys. Rev. C **65** (2002) 054909 [arXiv:nucl-th/0201038].

Table 2: Kinetic  $J/\psi$  formation at the LHC assuming both thermal charm momentum (left-hand side) and  $\Delta y = 4$  (right-hand side).

	$N_{J/\psi}$ (Thermal) $N_{c\bar{c}}(0)$			$N_{J/\psi} (\Delta y = 4)$ $N_{c\bar{c}}(0)$		
$b$ (fm)	200	150	100	200	150	100
0	52.7	32.5	16.4	17.5	10.8	5.48
1	50.5	31.2	15.8	16.8	10.4	5.25
2	44.8	27.7	14.0	14.9	9.21	4.65
3	37.0	22.9	11.5	12.3	7.62	3.82
4	28.6	17.7	8.73	9.54	5.89	2.90
5	20.7	12.7	6.05	6.90	4.23	2.01
6	13.8	8.32	3.72	4.61	2.77	1.24
7	8.28	4.71	2.14	2.76	1.57	0.71
8	4.10	2.36	1.10	1.36	0.79	0.37
9	1.78	1.04	0.50	0.59	0.35	0.16
10	0.65	0.39	0.19	0.22	0.13	0.064
11	0.19	0.12	0.063	0.065	0.040	0.021
12	0.048	0.032	0.018	0.016	0.010	0.006
13	0.011	0.0078	0.0049	0.0037	0.0026	0.0016
14	0.0026	0.0019	0.0012	$8.6 \times 10^{-4}$	$6.3 \times 10^{-4}$	$4.1 \times 10^{-4}$
15	$5.9 \times 10^{-4}$	$4.4 \times 10^{-4}$	$2.9 \times 10^{-4}$	$2.0 \times 10^{-4}$	$1.5 \times 10^{-4}$	$9.7 \times 10^{-5}$